Int J Intell Robot Appl (2017) 1:124–142
DOI 10.1007/s41315-017-0016-8

REGULAR PAPER

Using an environmentally benign and degradable elastomer in soft robotics

Stephanie Walker[1,3] · Jacob Rueben[2] · Tessa Van Volkenburg[2] · Samantha Hemleben[3] · Cindy Grimm[3] · John Simonsen[4] · Yiğit Mengüç[3]

Received: 21 November 2016 / Accepted: 20 March 2017 / Published online: 11 April 2017

Abstract This work introduces an environmentally benign and degradable elastomer, poly(glycerol sebacate) with calcium carbonate (PGS-$CaCO_3$), for use in soft robotics. Development of greener materials like PGS-$CaCO_3$ contributes to robot designs that do not require retrieval and can safely degrade in the natural environment. A simplified synthesis method of PGS was used to create elastomer sheets, which were laser cut/rastered then laminated with cyanoacrylate glue into pneumatic soft actuators. The modified polymer synthesis method is accessible for roboticists and the three chemicals used are non-hazardous and inexpensive. Three accordion-style pneumatic actuators (3, 4 and 5 chambers) were characterized for free displacement and blocked force in both linear extension and curling motions, and an additional four 3-chambered actuators were also tested to leakage and failure. Material characterization of PGS-$CaCO_3$ samples of all ages gave: ultimate tensile strength (UTS) from 48 to 160 kPa, elongation percent at UTS from 157 to 242%, moduli from 45 to 154 kPa, average resilience of 88% at 100 cycles, and maximum compressive force of 246 N at 50% strain. After being in an approximately 50–55 °C compost pile for 7 days, the polymer visibly degraded and had an average mass loss of 20% across 12 samples. PGS's strength, elasticity, biodegradability and chemical safety make it a desirable option for roboticists looking to leverage sustainable materials. PGS may also prove a potential green alternative for robotics applications in ubiquitous environmental and infrastructure sensing.

Keywords Elastomer · Green chemistry · Soft robotics · Actuator · Degradable

1 Introduction

SOFT ROBOTICS AS A BURGEONING FIELD exploits the new material properties available in elastomers (Rus and Tolley 2015). Bioinspired soft robot designs rely on these elastomers to actuate, grab, envelop and otherwise deform to perform tasks. The intersection of materials science and soft robotics is especially valuable considering that many already existing elastomers can be incorporated into soft robot production (Li et al. 2012). Green technology development has many well-known benefits including reducing damage to environmental and human health and reducing nonrenewable resource use (Anastas and Warner 1998). Green design for robotics in particular has the additional benefit of introducing a wider variety of robotic materials for a larger array of tasks. Incorporation of degradable materials into a robotic device increases its ability to be deployed where retrieval of the robot is impossible. High-volume environmental data collection (Valdes et al. 2012), microsurgery (Breger et al. 2015), precision agriculture (Mulla 2013; Suprem et al. 2013),

Electronic supplementary material The online version of this article (doi:10.1007/s41315-017-0016-8) contains supplementary material, which is available to authorized users.

✉ Stephanie Walker
walkers@oregonstate.edu

[1] Materials Science, Oregon State University, 204 Rogers Hall, Corvallis, OR 97331, USA

[2] Chemical Engineering, Oregon State University, 116 Johnson Hall, Corvallis, OR 97331, USA

[3] Robotics, Oregon State University, 204 Rogers Hall, Corvallis, OR 97331, USA

[4] Wood Science and Engineering, Oregon State University, 120 Richardson Hall, Corvallis, OR 97333, USA

and dangerous location exploration (Muscato et al. 2012; Murphy et al. 2012) will all benefit from greener materials in robotics. Green elastomer development for soft robotics, however, has been lacking. Soft robotics faces the challenge of finding degradable elastomers that function well under repeated deformation and can be fabricated quickly, in addition to having accessible chemistries for roboticists. Current soft robot materials include off-the-shelf soft silicone rubbers (Rus and Tolley 2015), polyurethanes (Ho et al. 2011; Bauer et al. 2014) and acrylic foam tapes (Shankar et al. 2007; Shian et al. 2015). In terms of temporary robotics, all have issues with low degradability, difficult customization, or hazardous chemistries if the roboticist wishes to synthesize their own material. Knowing inherent hazards in chemical syntheses as well as degradability of the final polymer are important when creating soft robots designed for temporary use. Silicone elastomers can degrade chemically (Laubie et al. 2012), especially at high temperatures (Ratner et al. 2004) but are considered non-degradable polymers in medical technologies, where they are commonly used (Saltzman 2004; Dow Corning 2017; Fu and Kao 2010; Saltzman 2001). Ecoflex (Smooth-On) cured silicones are also not biodegradable according to a representative from the company. Polyurethane syntheses can require toxic isocyanates (Han et al. 2014), and acrylic acid monomers can be explosive (The Dow Chemical Company 2014). Incorporation of additives into PDMS to change its final structure has given very interesting results (Mac Murray et al. 2015), but material possibilities can still be expanded through inclusion of other elastomers in soft robot fabrication. Greener materials have the potential to reduce safety concerns during more in-depth robot material customization while increasing biodegradability. The transition, however, is not so simple. Making custom elastomers can require investment in chemistry equipment, and have complicated syntheses not necessarily accessible for a robotics lab (Guan et al. 2002; Nijst et al. 2007; Kharaziha et al. 2013). The balance of ease of manufacture with green material creation must be struck when incorporating materials science into the more mechanical engineering-focused field of robotics. Nevertheless, there are current synthesis methods that can be performed by roboticists in order to bring customizability and creativity to the elastomer material design, one of those being poly(glycerol sebacate) or PGS.

In this paper we introduce green chemistry techniques for the synthesis and fabrication of a soft robot material (Fig. 1). We select a promising candidate material first introduced as an implantable biodegradable elastomer (Wang et al. 2002), poly(glycerol sebacate) with an additive of calcium carbonate (PGS-$CaCO_3$). We outline the materials and methods to synthesize PGS-$CaCO_3$ from its raw constituents with a minimum of equipment and develop fast fabrication techniques for pneumatic actuators. We evaluate actuators and mechanical properties of the green elastomer under static, cyclic and compressive loading conditions as well as discuss the elastomer's degradability.

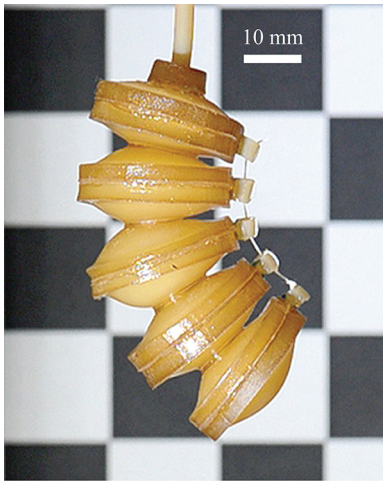

Fig. 1 PGS-$CaCO_3$ assembled into pneumatic actuators by laser cutting and adhering layers together

2 Background and related research

2.1 Soft pneumatic robots

Pneumatic actuation remains the most common actuation mode for soft robots. Pneumatic muscles consisting of a bladder with braided outer shell were first developed by McKibben in the 1960s (Committee on Prosthetics Research and Development 1961; Ilievski et al. 2011). Strategic placement of where the elastomer will deform defines locomotion. These actuators can mimic biological motion of soft creatures like caterpillars, sea slugs, and octopi as well as tongues and elephant trunks (Kier and Smith 1985). Some examples of pneumatically actuated soft robots include quadrupeds (Shepherd et al. 2011), grippers (Ilievski et al. 2011; Stokes et al. 2014), tentacles (Martinez et al. 2013), modular soft robots (Morin et al. 2014a, b) and muscle forms in general (Chou and Hannaford 1996; Davis et al. 2003). Pneumatic soft robots have also been suggested for medical use like the Colobot (Chen et al. 2013) for colonoscopy surgery, and a swallowing robot for patients with dysphagia (Chen et al. 2014). One limit to the performance of these robots is possible slow expansion, which can be improved by reducing the required volume of gas needed for actuation (through structural geometry) as well as tuning material compliance (Mosadegh et al. 2014) or wall thickness.

2.2 Degradable robots

Environmentally-friendly robotics research has employed a variety of degradable materials: a biodegradable miniature gripper for surgery (Breger et al. 2015), biodegradable and edible gelatin actuators (Chambers et al. 2014), robotic scaffolds for tissue engineering (Stoica 2009), a degradable origami robot (Miyashita et al. 2015), proposed biodegradable caterpillar robot (Trimmer et al. 2012), and a microrobot for drug delivery (Fusco et al. 2014). While biodegradable rigid materials are relatively well explored, more work is needed in the field of soft green elastomers in robotics. Natural rubber is the most commercially available polymer, but has not seen a lot of use in soft robots.

2.3 Green elastomers

Biodegradable elastomers potentially used for soft robotics include natural rubber, PGS, polycaprolactone (Thomas and Nair 2011), poly(vinyl alcohol) hydrogels (Xu et al. 2014), poly(1,8-octanediol-*co*-citric acid) (Yang et al. 2004), and others. Poly(glycerol sebacate) (PGS) is a tough biodegradable elastomer first introduced for potential applications in medical devices (Wang et al. 2002). The synthesis of this elastomer includes a melt under nitrogen flow and curing step under vacuum with sebacic acid and glycerol monomers (and typically no solvents). Ideal synthesis of PGS produces water and the polymer itself with no chemical waste beyond solvents and/or soap used to clean glassware.

Green chemistry principles and analysis suggest that PGS production and use could be more sustainable than current common elastomers (silicones, polyurethanes, acrylic adhesives). PGS monomers come from renewable resources (sebacic acid from the Ricinus communis (castor oil) plant (Ogunniyi 2006), glycerol potentially from vegetable fats and oils (Quispe et al. 2013)). Though the calcium carbonate additive is likely mined, it is a natural substance that makes up shells and bones and is only harmful when concentrated (Oregon 1998). Biodegradation of PGS occurs via "surface degradation by cleavage of ester linkages" (Rai et al. 2012). Under animal skin PGS disappears within 60 days (Wang et al. 2002). After breakage of its ester bonds, PGS has acidic degradation products (Liang et al. 2012; Chen et al. 2010) that can be toxic to cells. But, sebacic acid has an NFPA hazard rating less than or equal to vinegar (depending on the supplier of the vinegar) (Global Safety Management 2014b; Sebacic Acid Material Safety Data Sheet 2015; Flinn Scientific, Inc. 2012), and it is a component of a natural metabolic process in the body (Wang et al. 2002). PGS degradation has not been extensively studied in the environment so it is difficult to say how fast it will degrade, but glycerol components are readily taken up by microorganisms (Dobson et al. 2012), and calcium carbonate is already present in the environment (Oregon 1998). Inclusion of a basic additive (Bioglass) (Liang et al. 2012) in PGS has been suggested as an option to lower the toxicity of acidic degradation products through acid/base neutralization. Sebacic acid polymers and glycerol are also approved by the US Food and Drug Administration for medical use (Wang et al. 2002) and have low health, fire and reactivity hazard ratings (Sebacic 2015; Glycerol MSDS 2016; Avantor Performance Materials, Inc. 2014a).

PGS has been polymerized with various additives for: tuning biodegradation [(glycolic acid (Sun et al. 2010)], tissue engineering research [gelatin (Kharaziha et al. 2013)] [poly(ethylene glycol) (Patel et al. 2013)], and creating photocurable elastomers [acrylates (Nijst et al. 2007)]. PGS can also be cured in different amounts of time in order to control crosslinking and therefore mechanical properties (Jaafar et al. 2010; Chen et al. 2008). Rai et al. (Rai et al. 2012) reports that PGS has an "average tensile Young's modulus between 0.0250–1.2 MPa, UTS greater than 500 kPa, and strain to failure greater than 330%," although even greater elongation at failure, 550%, was observed with an addition of Bioglass (Liang et al. 2010). Bioglass (45S5) is a mixture (by weight) of "45% silica (SiO_2), 24.5% calcium oxide (CaO), 24.5% sodium oxide (Na_2O), and 6% phosphorous pentoxide (P_2O_5)" (Krishnan and Lakshmi 2013). It is a degradable bioceramic (Liang et al. 2010) that bonds with bone and stimulates bone growth (Jones 2013). In Liang et al. (2010), it was hypothesized that the calcium carboxylate groups are the primary contributor to the extreme elongation of Bioglass-PGS via ionic crosslinking. To try to improve elongation of our PGS polymer, we used calcium carbonate as an additive because it is an abundant natural material and safe enough to use as a food supplement (Oregon 1998). Calcium carbonate is expected to react with the ends of the sebacic acid to produce calcium ions and carbon dioxide gas, though the extent of reaction between $CaCO_3$ and sebacic acid for was not determined for this paper. The strength of the final polymer could be improved by such ionic crosslinking. If the robot spends the bulk of its time underwater, the calcium might dissociate, which would reduce the crosslinking effect and decrease the modulus of the polymer (Liang et al. 2010).

3 Materials and methods

3.1 Synthesis and assembly of PGS-$CaCO_3$ actuators

Glycerol (Fisher Scientific) and sebacic acid (Sigma Aldrich, 99%) were melted in a 0.16:0.16 molar ratio with

1 wt% of calcium carbonate (J.T. Baker, 99.0%) between average temperatures of 134 and 139 °C in a 250-ml round-bottom flask for 24 h under approximately 100 ml/min nitrogen flow. Stirring was set to level 1 on the hot plate. The melt (pre-polymer) was then poured onto a clean PTFE-coated liner set in a metal baking pan and cured at average stage temperature of 137–143 °C in a vacuum oven (50.8 kPa) for 10–11.25 h (Fig. 2). For more detailed temperature information see Online Resource 1. Crosslinking was not controlled after curing beyond taking the sample out of the oven. Temperature of the melt varied slightly because of changes in room temperature. Because the melt was in a hood, the air flow affected the heat transfer between the aluminum flask holder and the polymer melt.

Samples were coated with corn starch and/or olive oil to reduce stickiness during fabrication. The approximately 3-mm thick sheets were then laser cut and/or rastered into either dumbbell, disk, or actuator shapes. Cutting was performed with two passes on a VLS4.6 Universal Laser Systems Laser Cutter (60 W) at 50% power, 5% speed, 1000 PPI, and with the 2.0 lens, with the laser focused at the bottom of the polymer. Rastering was performed at 50% power, 30% speed, 1000 PPI with the laser focused at the bottom of the polymer. Rastering creates height differences in the actuator pieces for a more defined glue boundary. The focal point of the laser was the bottom of the polymer to accommodate the varying height of the samples (approximately 2.6–3.8 mm). Any crosslinking after fabrication was not studied in this work.

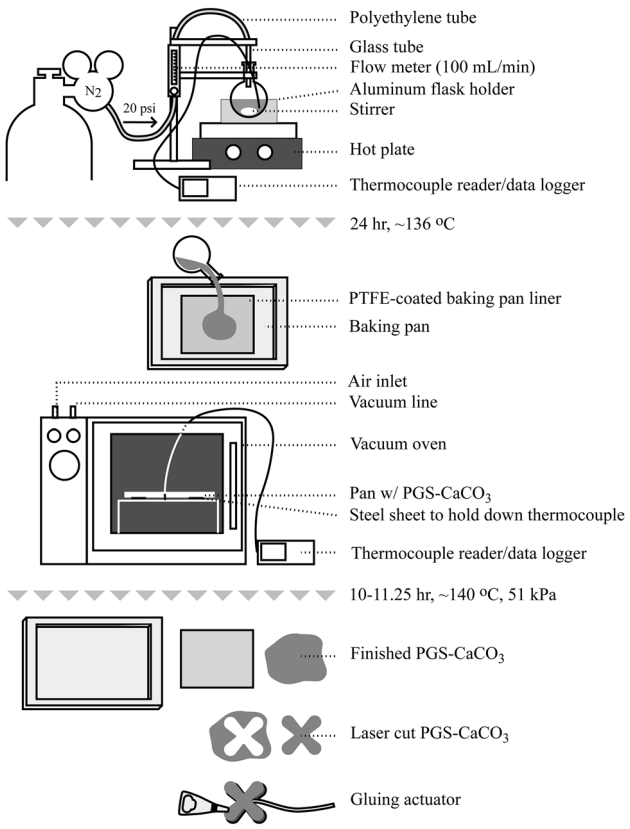

Fig. 2 Synthesis of PGS-$CaCO_3$ includes a melt step and a cure step followed by laser cutting, rastering and gluing the polymer sheet to create a robot actuator

The laser cut and rastered circular layers (25 mm diameter) were laminated into actuators using a approximately 1 mm bead of cyanoacrylate gel glue (Loctite Super Glue Ultra Gel Control). The raised edges of the layers reduced the spreading of the glue to undesired parts of the actuator. The rastered away portions of the layers created air gaps for the actuator chambers. Latex tubing was cut into approximately 3 mm long beads and glued to the actuator to make a spine for tying a cotton thread to make a strain-resistant side (Fig. 3). For comparison, three actuators were made out of Ecoflex 00-30 (one of each of 5-, 4-, and 3-chambered) using a similar process. Ecoflex 00-30 was poured into molds with the same dimensions as the laser cut PGS-$CaCO_3$, degassed for 3 min and cured in a 40 °C oven for 30–60 min. The components were then laminated together using Sil-Poxy (Smooth-On). Tubing (non-latex) was then attached in a similar way as previously described.

3.2 Actuator testing (extension, force, peeling, leakage)

Free extension for 5-, 4-, and 3-chambered actuators (Actuators A, B and C) was measured under air pressure in 0.34 kPa increments. Inflation pressures were chosen so that leaking or breakage could be avoided for the PGS-$CaCO_3$ actuators. Extension was measured once for curling and straight actuation. Actuator elongation lengths were measured manually with the pen tool in Adobe Illustrator. Free extension was also measured for two additional 3-chambered actuators, one actuator for straight extension (Actuator D) and one actuator for curling extension (Actuator E), until leakage and then to failure. Elongation percents and pressures at leakage and break were recorded. Ecoflex actuators were not tested for leakage and failure.

Actuator blocked force was measured once for each actuator for both curling and straight pneumatic actuation using an Ohaus Scout Pro mass balance. One side of the actuator was set against a stationary clamp and the other was lightly set on the scale. For straight blocked force the actuator was placed directly on the scale. For the curved blocked force the actuator tip was placed lightly on the scale. The Ecoflex actuators were also subjected to straight and curved blocked force tests. Mass readings were multiplied by 9.81 m/s^2 to get force values. Blocked force and

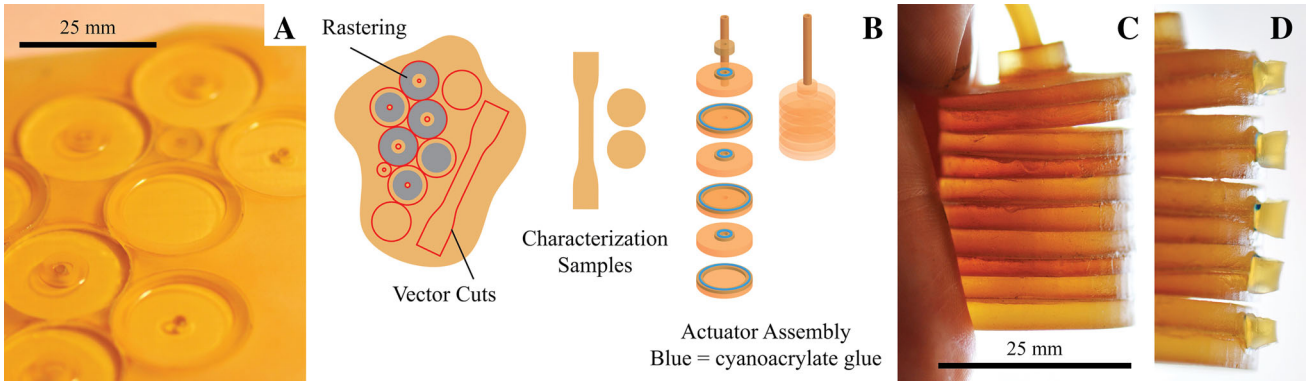

Fig. 3 **a** The PGS-$CaCO_3$ sheet was laser cut and rastered to create actuator components which were laminated together with cyanoacrylate glue. Rastering the polymer sheet gives control over thickness of the polymer layer and was used to create raised edges for gluing. **b** Diagram of laser cutting plan for each PGS-$CaCO_3$ sheet. Both vector cuts and rastering were used to create 25 mm circular disks for laminating into a 3-, 4-, or 5-chambered pneumatic actuator. **c** A 5-chambered pneumatic actuator in a neutral position. **d** Pieces of 1/8" outer diameter amber latex tubing approximately 3 mm long were glued to one side of the actuator so a cotton thread could be tied to create a strain resistant layer

pressure at leakage and failure were also recorded once for two additional 3-chambered actuators (for curling (Actuator F) and straight (Actuator G) blocked force).

Peeling between adhered PGS-$CaCO_3$ layers was tested with 10 commonly available glues. Two 20 × 5 mm strips of the polymer were adhered together with one polymer also attached by cyanoacrylate glue to a tongue depressor. Experimental glues were applied between samples and left overnight to dry. Two pieces of wood were cut and adhered with cyanoacrylate glue to the other polymer end where a bag was hung to gather incremental mass increases. The glue that held the most mass before delamination of the two PGS-$CaCO_3$ layers was chosen for fabrication.

Leakage in the actuators was determined by inflating Actuators A, B, and C to their maximum testing pressure with a syringe and clamping the syringe position (6.9 kPa for Actuators A and B and 3.45 kPa for Actuator C). The change in pressure over the first 30 seconds was determined once for each actuator. Leakage is also noted in elongation and blocked force data for Actuators D, E, F, and G.

3.3 Tensile and cyclic testing

Tensile tests were performed on dumbbell samples using a Mark-10 Tensile Tester (25 N load cell) with extension rates of 100 mm/min and 500 mm/min. Dumbbell samples were based on the dimensions laid out for Die D in ASTM D412 (original parameters from ASTM D412 Die D: height 16 mm ± 1 mm, width 100 mm minimum, gauge length 33 ± 2 mm, large curvature radius 16 ± 2 mm; parameters from PGS dumbbell vector: height 16.5 mm, width 101.6 mm, gauge length 33.7 mm, large curvature radius approximately 16 mm). The tensile testing speed of 500 mm/min was used to adhere to the lower bound ASTM D412 speed designation. Samples were also run at 100 mm/min to replicate a slowly expanding robot. Sandaper pieces (approximately 17 mm × 20 mm) were glued with cyanoacrylate adhesive (Loctite Super Glue Ultra Gel Control) to both sides of the ends of the dumbbell shapes to reduce slipping during testing. Stress versus elongation percent data of approximately one day old PGS-$CaCO_3$ samples tested at 100 and 500 mm/min and three older samples at 500 mm/min are plotted. To explore relationships between material properties and processing conditions, moduli and UTS of samples of all ages (11 total) are plotted versus melt temperature, thickness, and age. Modulus was determined using the average slope of each sample for the first 10% of the stress vs. elongation % graph. Moduli from all approximately one day old samples is plotted versus elongation percent to observe nonlinearities. Tensile tests (500 mm/min and 100 mm/min) were also performed on four samples of cured Ecoflex 00-30 and 4 samples of cured natural latex rubber (from Liquid Latex Fashions, poured and dried in air). The same dumbbell vector as the PGS-$CaCO_3$ samples was used to create molds. One representative curve from each material at both speeds is plotted with PGS-$CaCO_3$ to compare material properties.

Cyclic loading tests were also performed on approximately 1-day-old dumbbell samples using a Mark-10 Tensile Tester (25 N load cell) with an extension rate of 500 mm/min. Samples were pulled to 60% elongation and released at 500 mm/min for 100 cycles. Hysteresis behavior is shown in a stress vs. elongation % plot. Resilience (the percent of energy not lost to hysteresis) is calculated using cycle 100 data with areas under the loading curve (A_L) and unloading curve (A_U) (Bellingham et al. 2003) (Eq. 1).

$$\text{Resilience}\,\% = (1 - (A_L - A_U)/A_L) \times 100\%. \quad (1)$$

3.4 Degradation analysis

Degradability was tested in a cattle waste hot compost (approximately 50–55 °C). Samples (25 mm diameter, 4 and 0.5 days old) were sewn into fiberglass (screen door material) mesh bags with fishing line, weighed (sample, line and bag), and then buried 24 inches deep into the compost. After seven days, each sample was removed from the compost, shaken in a bottle with deionized water for 10 min to remove debris, and set in a 35 °C oven to dry for 24 h. A degradation timeline of one week was selected as a starting point in order to get a general idea of degradation in a short time. Samples were dried for one day in order to get rid of excess water that would change the mass of the elastomer. The dried samples in the mesh bags were weighed and mass loss was calculated for each. A fresh polymer sample surface is compared to its "after" photo in the mesh bag. Mesh bags were inspected to ensure that no fishing line had broken (no samples slipped out).

4 Results

4.1 Actuator testing (extension, force, peeling, leakage)

Images of actuator A, B, and C extensions (straight and curved) as well as measurement methods are presented in Fig. 4. Actuator elongation percents and blocked force values for both curling and straight pneumatic actuation for Actuators A, B, and C are presented in Fig. 5. Results from the characterization of Ecoflex 00-30 actuators are included for comparison.

Elongation percent per pressure input in the PGS-$CaCO_3$ actuators increased as the number of chambers decreased. This could be due to slightly varying material properties across actuators. The PGS-$CaCO_3$ 5- and 4-chambered actuators also showed a decreasing elongation percent increase as the pressure was increased, seemingly due to reaching the limits of the amount of extendable material (cyanoacrylate glue makes the edges stiffer). The curved PGS-$CaCO_3$ actuators behaved similarly but with elongation percents mostly exceeding the straight actuators. The elongation percents for straight actuators ranged from approximately 39–49 elongation percent, and for curved actuators 46–48 elongation percent. The Ecoflex 00-30 actuators performed in a similar elongation percent range but did not display the extendable material limit behavior shown in the PGS-$CaCO_3$ samples. The Ecoflex samples did show a more linear trend for elongation percents with higher elongation than across most PGS-$CaCO_3$ actuators. This is expected because the Ecoflex 00-30 and Sil-Poxy adhesive actuators are softer overall than PGS-$CaCO_3$. Because of the manual nature of fabrication, Ecoflex 00-30 actuators were not entirely identical, which may have led to some variation in actuator performance. Even so, the data show expected trends (due to softness of the materials) for most actuator tests.

Straight blocked force for all three PGS-$CaCO_3$ actuators overlapped in an almost linear trend. Maximum force of 1.07 N came from Actuator B. Curved blocked force showed a similar trend up to about 4.8 kPa when Actuator A began to apply less force. This could be from the 5-chamber actuator's ability to expand more in the middle and curl instead of press on the mass balance plate. The maximum force (0.4 N) was again from Actuator B. The straight blocked force was smaller overall for the Ecoflex actuators, especially at the higher pressures. This makes sense from the Ecoflex 00-30 tensile testing data, which shows it has a smaller modulus than PGS-$CaCO_3$. The Ecoflex samples, even when put together with the stiffer silpoxy adhesive, are still softer overall than the PGS-$CaCO_3$/cyanoacrylate combination. The curved blocked force for the Ecoflex actuators fell in line with the PGS-$CaCO_3$ data, probably due to the actuators having similar geometry, limited expansion space, and the low pressures in testing.

Results for Actuators D, E, F and G tested to leakage and then to failure are as follows. Pressures at leakage of these actuators were 16.9 kPa (straight 96% extension), 12.4 kPa (curved 93% extension), and 12.3 kPa (curved 0.21 N force). The straight blocked force test reached the limit of the scale (1.84 N at 12.5 kPa) before any breaking or leakage was detected. Pressures at failure of these actuators were 19.7 kPa (straight 106% extension), 17.2 kPa (curved 136% extension), and 30.8 kPa (curved 0.064 N force because of slipping). These actuator samples have an average melt temperature of 138 °C and an average oven temperature of 141 °C.

The best adhesive tested was the Loctite Super Glue Ultra Gel Control. When held together with Loctite Super Glue, the polymer broke before the glue debonded. Leakage for Actuators A, B, and C in the first 30 s of inflation was 0.21, 0.21, and 0.69 kPa, respectively. Leakage occurred at the points where the superglue adhered the two layers of the elastomer together. This was qualitatively observed by placing each actuator in an oil bath and inflating the actuator to approximately the same pressure as during testing. (An olive oil bath was used because the cyanoacrylate glue turned white in water.) Small bubbles came out of both the larger diameter glue zones as well as the smaller chamber connector glue zones. Increasing the glue area on the edges of the actuator chambers could

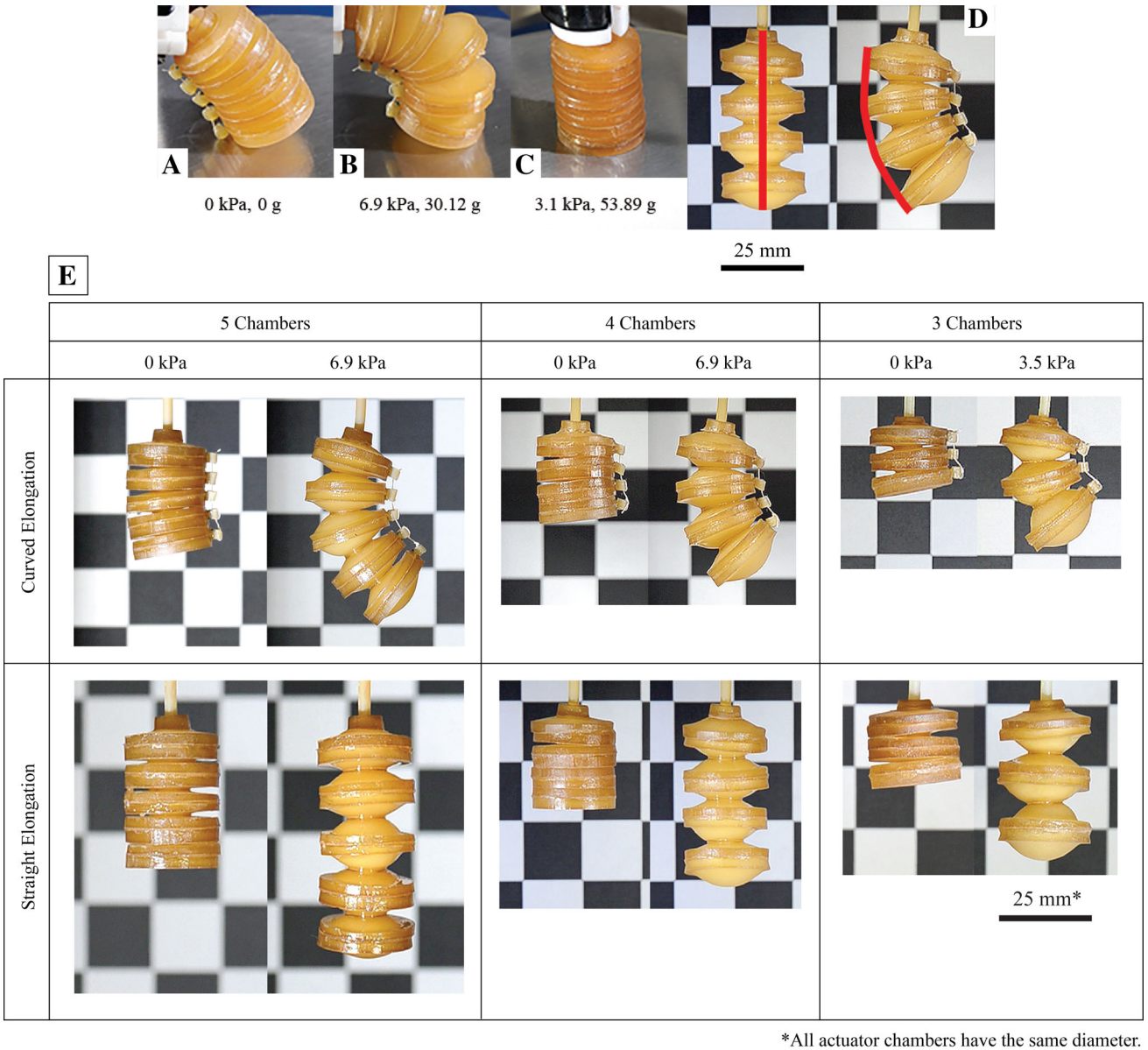

Fig. 4 **a**, **b** Placement of the actuator for curved blocked force at 0 and 6.9 kPa. **c** Straight blocked force at 3.1 kPa. **d** Elongation percent was measured using manually drawn line lengths in Adobe Illustrator. **e** Three accordion shaped pneumatic actuators (Actuators A, B and C, respectively) were inflated with 0.34 kPa increments of air and characterized for length of free extension in a straight and curled configuration

reduce leakage (the annulus for gluing was about 2 mm thick). We believe that the leakage has to do either with not enough surface contact between layers of PGS-$CaCO_3$ during gluing, possible chemical interactions with the elastomer and glue causing delamination, and/or cracking of the brittle glue layer during fabrication. We had some success with a flexible cyanoacrylate glue (Loctite Instant-Bonding Adhesive 4851), but its performance was irregular (layers delaminated upon actuation). More research into glues that are compatible with this chemistry will be worthwhile.

4.2 Tensile and cyclic testing

UTS at failure of the dumbbell samples ranged from 48 to 160 kPa. Elongation percent at UTS ranged from 157 to 242%. Moduli in the first 10% of data ranged from 45 to 154 kPa (Fig. 6). Overall, PGS-$CaCO_3$ behaves nonlinearly and some of the 500 mm/min and 100 mm/min samples overlap due to slight differences in temperature conditions or thickness. For the 500 mm/min tests, samples cut from the same sheet of polymer overlapped, but had different elongation percents at break. The 100 mm/

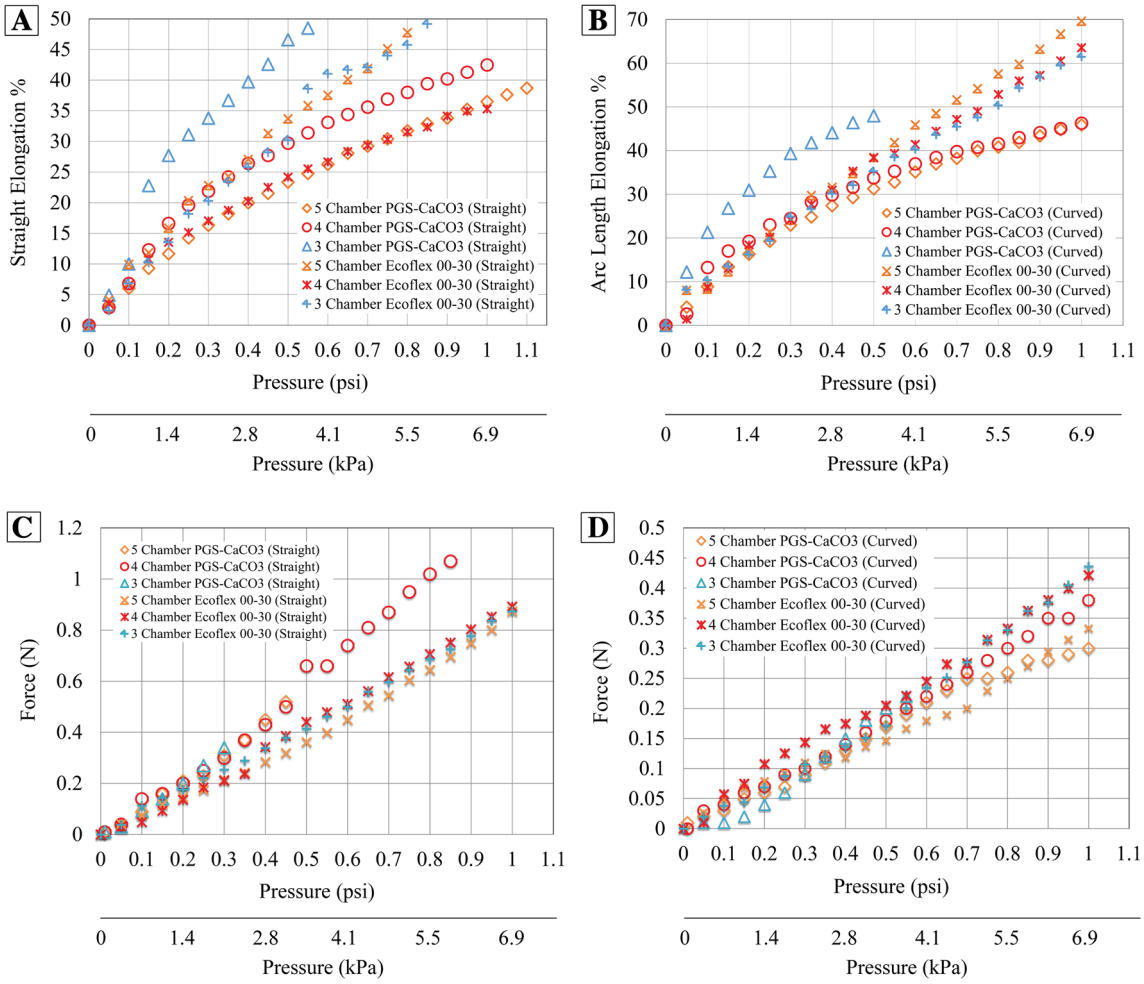

Fig. 5 **a** Elongation percent of straight free expanding actuators with applied air pressure. **b** Arc length elongation percent of curved free expanding actuators with applied air pressure. **c** Blocked force for straight chambered actuators. **d** Blocked force for curved chambered actuators. PGS-$CaCO_3$ elongation shows some stiffening behavior at higher pressures that is not seen in most actuators made using the softer Ecoflex 00-30/Sil-Poxy

min data had a pair of samples that overlapped from different runs. There is still too much variation within the same testing speed to see any trends based on elongation speed alone. In order to determine possible trends in the data, moduli of all the tensile samples were plotted versus: average melt temperature, sample thickness, and age (Fig. 7).

The differences in moduli seem to be related to melt temperatures and sample thicknesses. Cure temperature and time vs. moduli did not show any obvious trends. Observation of the polymer melt when it is poured into the baking pan shows that higher melt temperatures make the polymer more viscous and more likely to form long strands when poured (more polymer interactions are present). Sample age did not show any strong relationship to moduli. Moduli of the tensile samples also increase with an increase in strain rate. The range, average and standard deviation of moduli for samples tested at 100 mm/min were 45–123, 85, and 28 kPa, respectively. The range, average and standard deviation of moduli for samples tested at 500 mm/min were 58–154, 113, and 32 kPa, respectively.

PGS-$CaCO_3$ tensile testing modulus curves all have a similar structure where a higher slope occurs within the first 50% of elongation and then a bend occurs, moving towards a lower and more constant modulus (Fig. 8a, b). In plots of modulus vs. elongation %, a relatively constant slope is reached between 80% and 140% elongation. Tensile testing results for Ecoflex 00-30, natural latex rubber, and PGS-$CaCO_3$ are compared in Fig. 8c. Natural latex rubber is stiffer than PGS-$CaCO_3$ and has a large plateau where plastic deformation takes place. Only the 500 mm/min sample of PGS-$CaCO_3$ data was included because 100 and 500 mm/min PGS-$CaCO_3$ tensile tests gave overlapping data. Ecoflex 00-30 is less stiff than PGS-$CaCO_3$ and also more nonlinear.

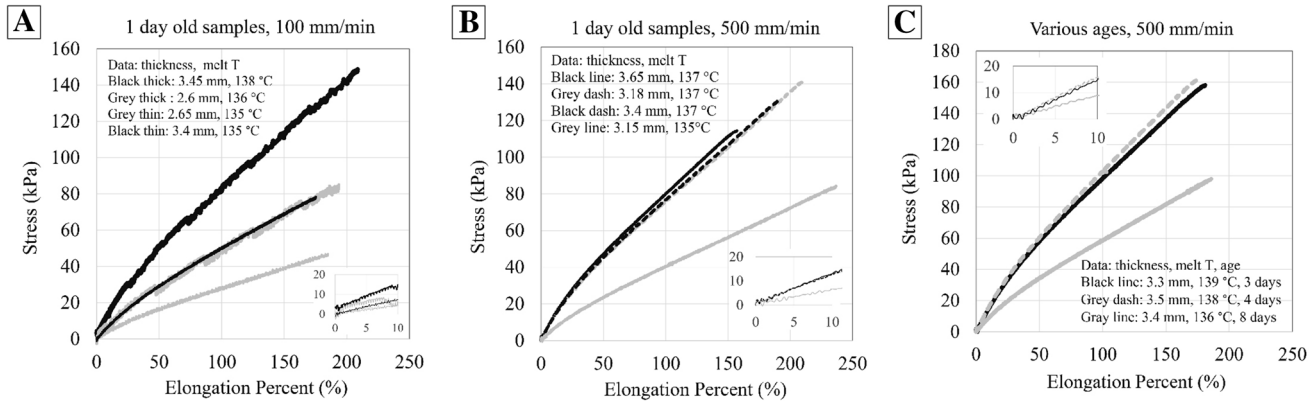

Fig. 6 Tensile testing of PGS-$CaCO_3$ samples of slightly varying processing conditions but similar ages (data in Online Resource 1). Tensile tests at **a** 100 mm/min testing speed on approximately one day old samples, **b** 500 mm/min testing speed on approximately one day old samples, and **c** 500 mm/min speed on aged samples were performed. UTS at failure of all dumbbell samples ranged from 48 to 160 kPa. Elongation percent at UTS ranged from 157 to 242%. Moduli in the first 10% of data ranged from 45 to 154 kPa. There is overlap between 500 and 100 mm/min curves

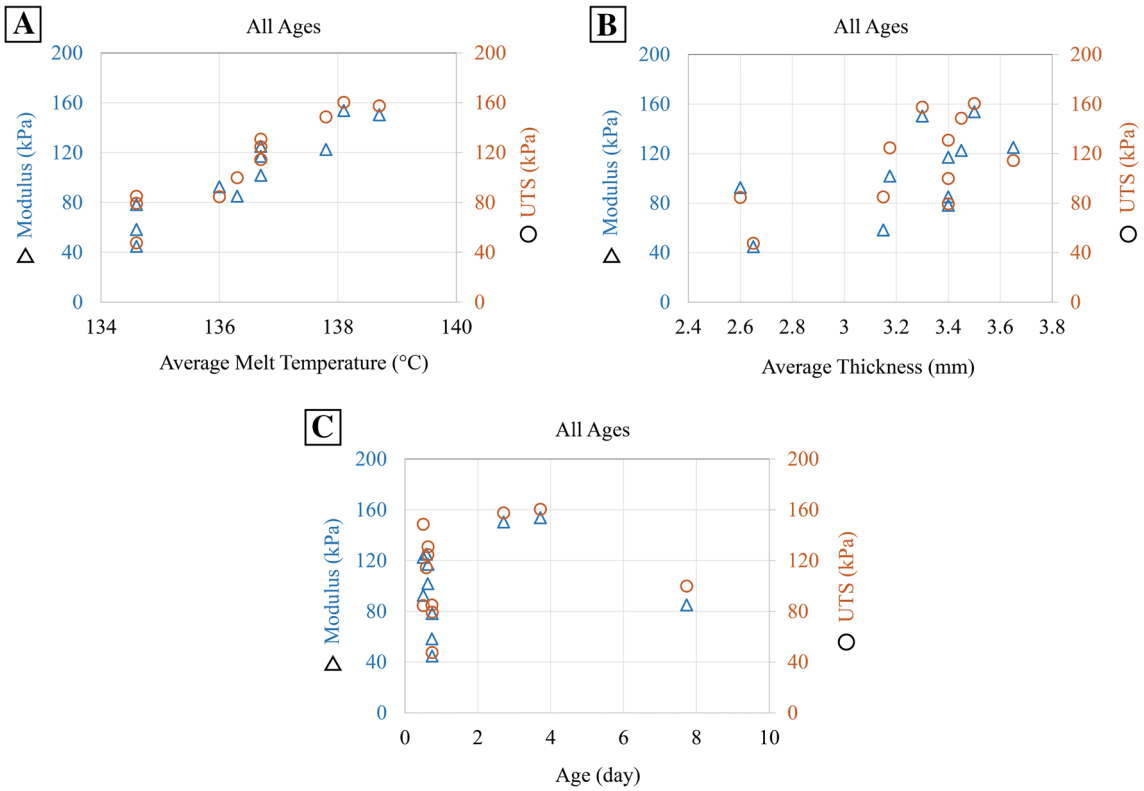

Fig. 7 **a** Moduli and UTS increase with increased melt temperature. **b** Moduli and UTS increase with increased sample thickness. **c** Age of the polymer does not show any clear relationship to moduli or UTS

Figure 9 shows three data sets from cyclic loading of PGS-$CaCO_3$ samples. The average resilience was 88% for the 100th cycle from all three samples tested with a standard deviation of 3%. Hysteresis occurs, showing that the polymer has some viscoelasticity. In the first cycle, the polymer is permanently deformed and then by the 20th cycle the polymer starts to settle into a repeating loop.

4.3 Degradation analysis

After seven days in the compost (Fig. 10a–c), some polymer samples had almost completely disappeared and some were relatively intact. Mass loss could be even greater in some samples if less wood and dirt became embedded in the polymer. Amount of compost contact could have been

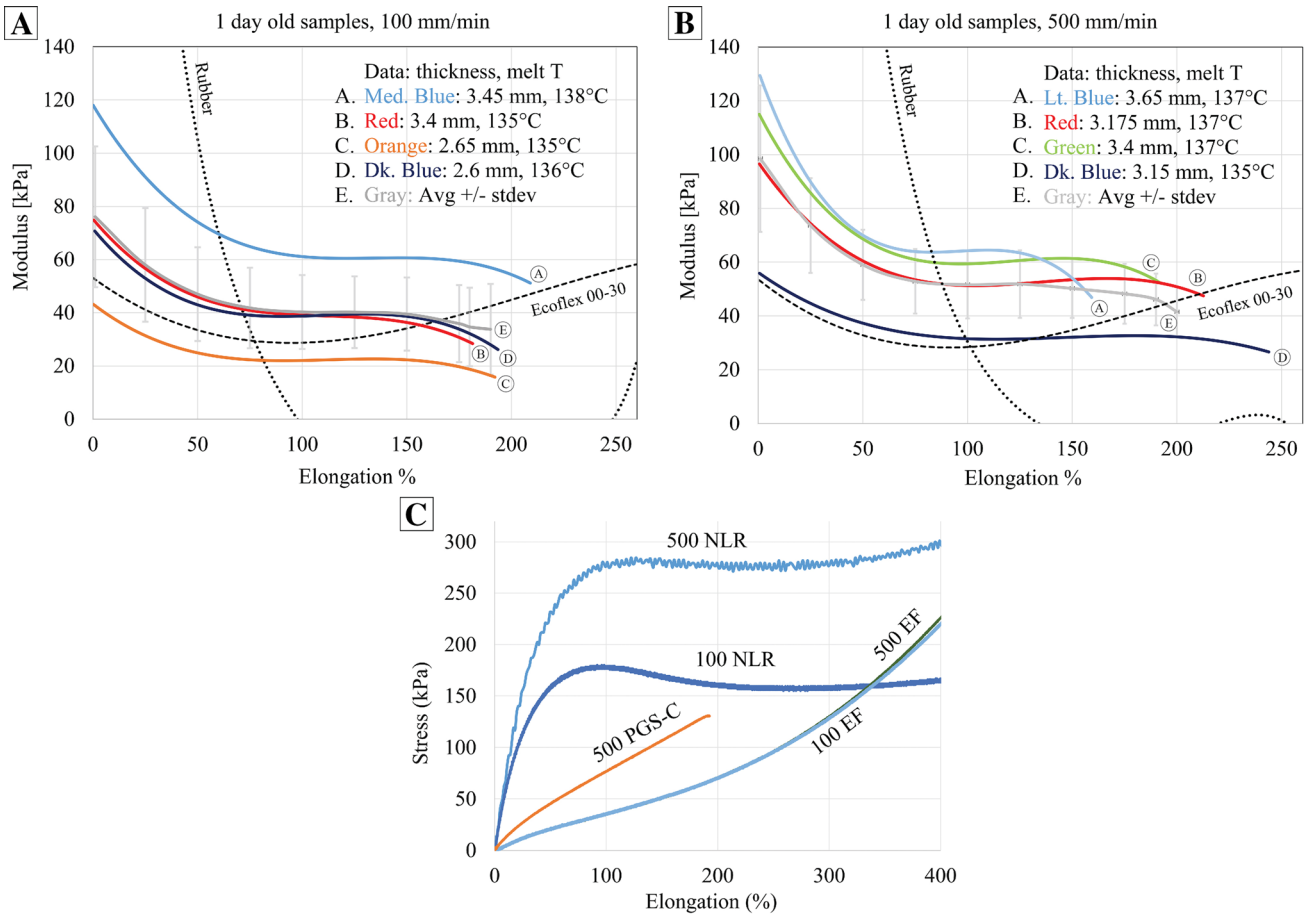

Fig. 8 Moduli versus elongation percents of PGS-$CaCO_3$ (and Ecoflex 00-30 and natural rubber for comparison) for same age **a** 100 mm/min and **b** 500 mm/min tensile data show the nonlinearity of PGS-$CaCO_3$, but a relatively constant modulus value is reached around 80% elongation and continues until approximately 140% elongation. **c** Tensile testing (500 mm/min = 500, 100 mm/min = 100) of PGS-$CaCO_3$ samples (PGS-C) compared to Ecoflex 00-30 (EF), a common silicone used in soft robotics, and natural latex rubber (NLR). PGS-$CaCO_3$ behavior is nonlinear. Ecoflex samples tested at different speeds overlap at these elongation percents. Natural latex rubber shows plastic deformation starting at around 100% elongation. Ecoflex 00-30 within 200 % elongation has lower moduli than most of the PGS-$CaCO_3$ samples. Rubber's maximum and minimum moduli are out of the range of the PGS-$CaCO_3$ samples

low for the intact polymers, as there was no way to ensure identical compost contact for each sample once they were buried. Also, even though there may have been anaerobic pockets in the compost, the degradation is expected to be aerobic. Further degradation testing will clarify degradation type. The best (70% loss) and worst case (4% loss) scenarios are shown in Fig. 10d (Sample 6 and A). Average mass loss across all samples was 20% with a standard deviation of 22% (Fig. 10e).

4.4 Possibilities for assembly, motion, and application

Lamination possibilities for PGS-$CaCO_3$ can include entire bodies of robots where the pneumatic actuators facilitate simple animal-like locomotion or simple grippers (Fig. 11a, b). A frog robot with a small hydraulic or pneumatic source could swim down onto a river bottom and and sample the soil for heavy metals. A gripper could be attached to a caterpillar-like robot to help it grip and climb trees and rocky faces. Application possibilities for robots made of PGS-$CaCO_3$ include those that can apply towards the DARPA VAPR and ICARUS programs (Roy Olsson 2017) that seek to develop self-destructive electronics and vehicles that vanish after critical supply deliveries. A PGS-$CaCO_3$ robot would degrade into the natural environment after being used as a component in a delivery vehicle, provided that the other components (electronics, power supply) could also disappear (Fig. 11c). PGS-$CaCO_3$ could also be applied to environmental sensing. As an example, the caterpillar-like robot that climbs trees could sense gases or contaminants in the air. At the end of its life cycle, it would fall to the ground and degrade into the soil. PGS's potential in medicine has been described in previous work, and by reducing acidic byproducts it may be possible to expand the range of PGS-$CaCO_3$ robots to apply to medical technologies like swallowable robots that deliver medication, for example.

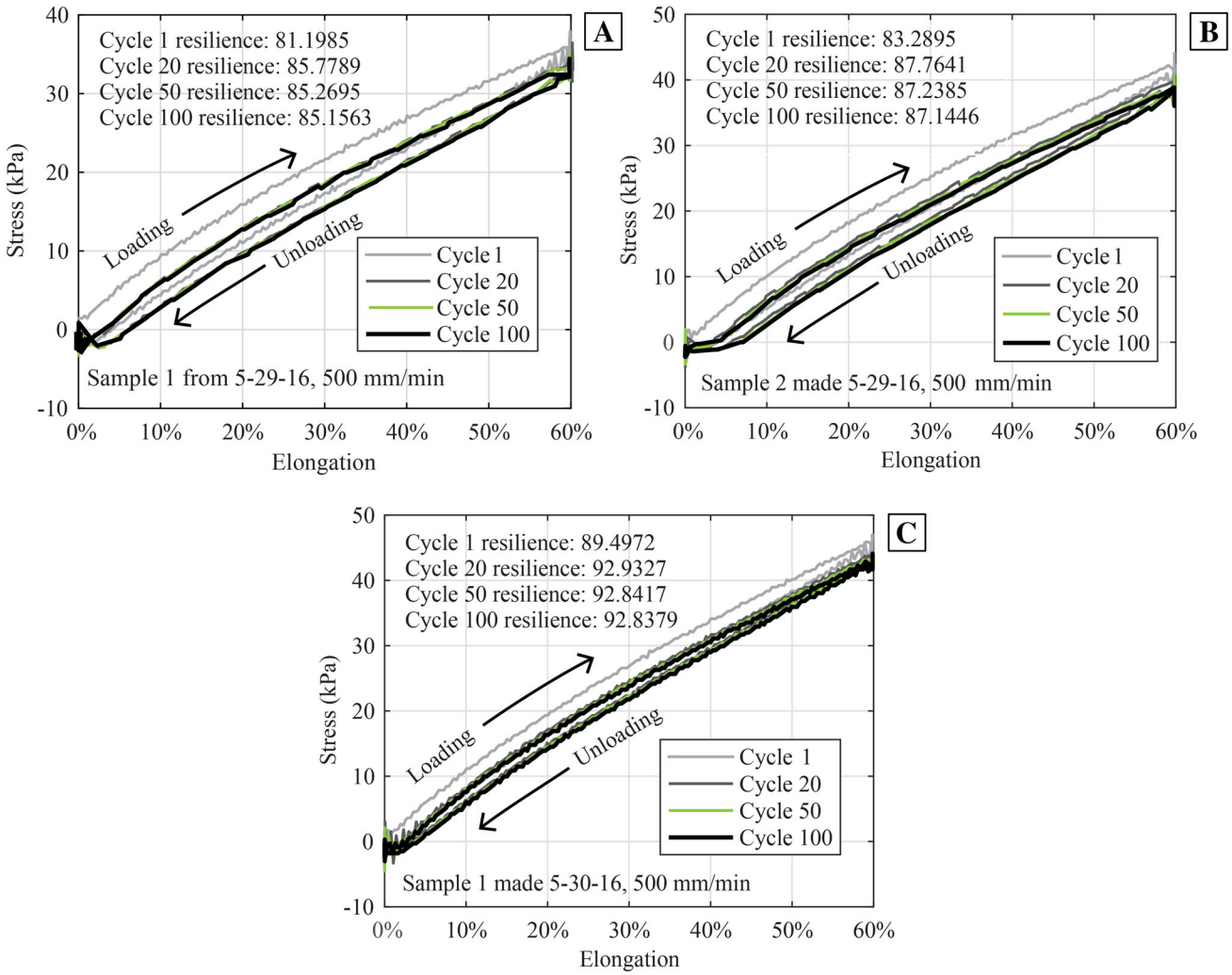

Fig. 9 Cyclic testing data from three samples less than a day old. Average resilience of the 100th cycle for the three samples tested was 88% with a standard deviation of 3%

5 Discussion

PGS-$CaCO_3$ seems to be a promising candidate for further exploration into soft robotics materials science. Both the actuator testing and tensile testing showed that PGS-$CaCO_3$ material properties are in the same ranges as commercially-available Ecoflex 00-30. While PGS-$CaCO_3$ is an exciting candidate to develop further, there are some issues to improve upon.

Settling of a thin layer of what is assumed to be calcium carbonate sometimes occurred after pouring the prepolymer melt, and cracking sometimes occurred during tensile testing at the $CaCO_3$-dense polymer bottom, so quicker cure times (to prevent the filler from settling after stirring stops) or less $CaCO_3$ would improve homogeneity. Filler composition will be explored in future work. The baking pan warped slightly during use, which could have partly caused the varying height of the sheets. Slight variations in polymer melt temperature are suspected as another cause of varying sheet thicknesses (due to varied viscosities and polymer chain lengths/structures). We also assumed that the thin layers of olive oil and corn starch coatings did not affect bulk material properties.

Elongation percent values of approximately 200% are desirable for soft robots, and PGS-$CaCO_3$'s tensile data fall between natural latex rubber and Ecoflex 00-30 values, but the actuation pressures of PGS-$CaCO_3$ need to be gentler than those made with high elongation silicones like Ecoflex because of PGS-$CaCO_3$'s lower elongation % at break. Variations in PGS-$CaCO_3$ stress/elongation % data seem to originate from slightly varying melt temperatures and thickness differences between samples. More PGS-$CaCO_3$ replicates should be run in a tightly controlled temperature and cure time range to

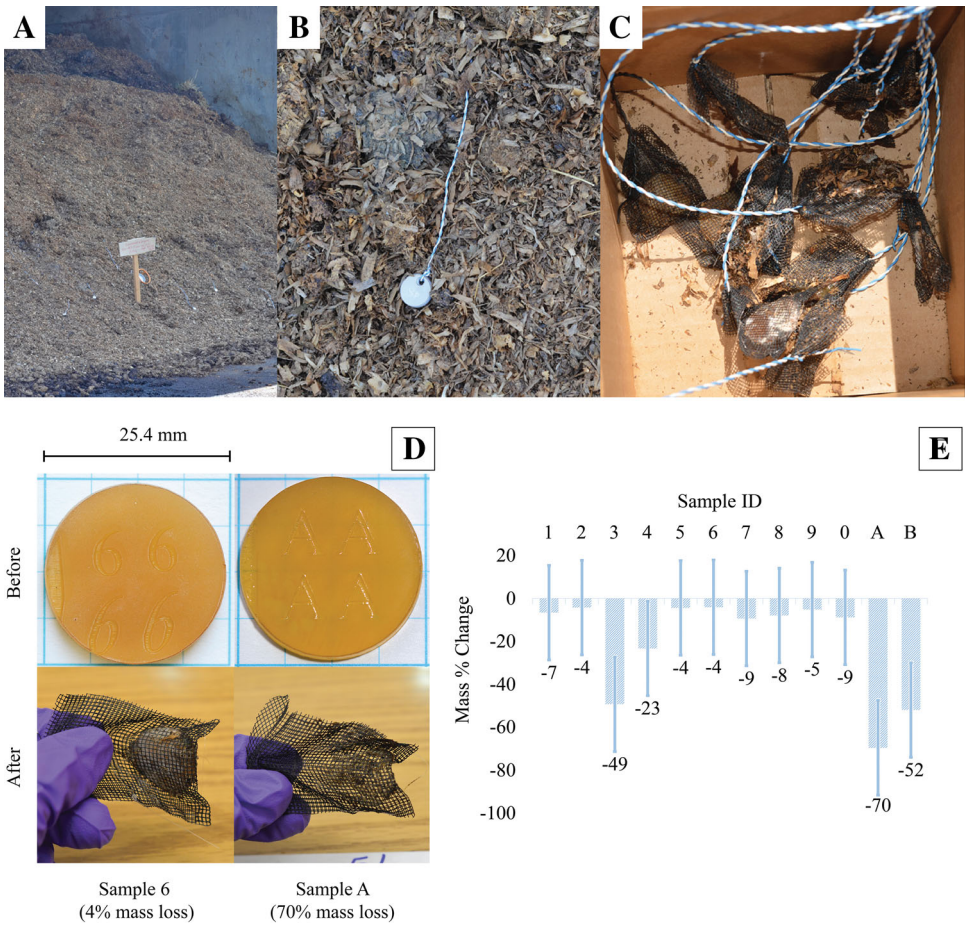

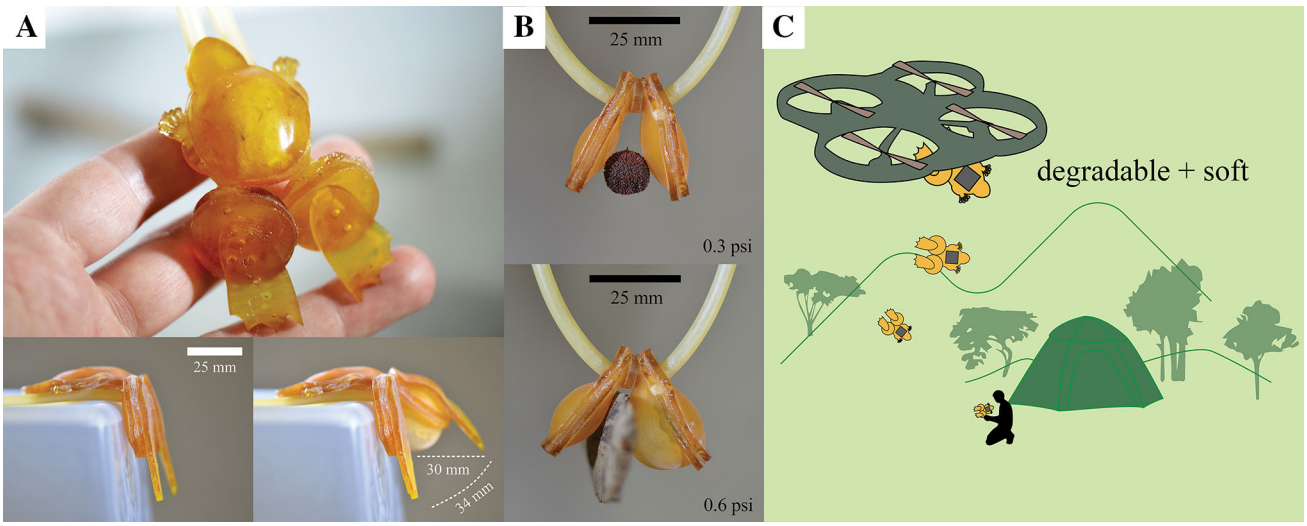

Fig. 10 **a** Location, **b** burial, and **c** packaging of samples for degradation. **d** Polymer samples 6 and A had the minimum (4%) and maximum (70%) mass loss after being taken out of the compost. Sample A was almost completely gone from the mesh bag. **e** Average mass loss across all samples was 20%, with a standard deviation of 22%. The mass loss might have been greater for some samples if debris from the compost were not embedded into the sticky polymer

Fig. 11 Possibilities for fabrication include **a** frog legs and **b** gripper actuators. **c** A possibility for application of a PGS-$CaCO_3$ robot fits well into the ideas laid out in the DARPA ICARUS program where a vehicle disappears after delivering critical supplies. Here we have used the frog as an example of a soft robot that can be dropped with a package and travel to a specified site, then degrade

narrow down moduli and elongation percent values. PGS-$CaCO_3$'s extension is close to smooth muscle (300%) (Li et al. 2012) and could function well as a biological tissue mimic in a robot.

Uneven oven temperature distribution, inhomogeneity of filler, or pre-straining while pulling the polymer off the mold could have also caused mechanical properties to vary within each sample. Using a larger vacuum oven or smaller

sheet size would reduce effects of uneven temperature distribution. Resilience results suggest that the polymer would still function well after 100 cycles of deformation, but hysteresis needs to be taken into account when designing pneumatic power systems. Viscoelastic effects, as evidenced by the hysteresis loop, cause the polymer to release energy as heat. The permanent stretching in the first few actuations of PGS-$CaCO_3$ will also need to be programmed into the robot control system. The tensile properties also appear to be strain rate dependent.

Once cured, we can see that the polymer is changing its opacity over a period of weeks, and this could be an indication of some further property changes. In the current state, the polymer is expected to perform during the time window of 8 days shown in the aged tensile data, though more replicates to confirm this are desired. From a control standpoint, the polymer property changes should be further characterized in the long term to make control of a robot made from PGS-$CaCO_3$ straightforward. Actuator construction can still be improved through automation (3D printing with some alterations in chemistry) and potential molding techniques. Manually making the actuators is not ideal and can introduce errors in gluing. More actuator testing is needed to fully understand the repeatability of the manual process. The glue cracking issue needs to be resolved through more involved study of interactions between glue and PGS-$CaCO_3$ chemistry. The cyanoacrylate glue was also too stiff for the PGS-$CaCO_3$/glue boundaries. More environmentally friendly and flexible glues will be explored.

To address any questions about the release of CO_2 (a greenhouse gas) during the synthesis of PGS-$CaCO_3$, a calculation has been performed assuming all $CaCO_3$ reacts. While dissociation of calcium carbonate in reactions with the sebacic acid can produce carbon dioxide, a roboticist can make 1000 small actuators out of PGS-$CaCO_3$ in exchange for driving one less mile in a small car (calculation in the Appendix).

6 Future work

Further chemical, polymerization and mechanical testing will be performed to clarify appropriate operation parameters for PGS-$CaCO_3$ robot use, long-term degradation, and time to failure. FTIR (Fourier transform infrared spectroscopy) will give a molecular footprint of the polymer. Polymer characterization—DSC (differential scanning calorimetry) and DMA (dynamic mechanical analysis) will help explain any melting points and glass transition temperatures as well as further explain viscoelastic behavior. Static light scattering will identify the average molecular weight of the pre-polymer (before curing) for comparison to literature and other elastomers. A three-neck flask and condenser setup for the melt step will determine completeness of reaction. Degradation will be characterized via surface erosion behavior with SEM (scanning electron microscopy). Biodegradation can be tested more thoroughly with gas capture techniques. The potential material changes over time need to be further characterized. Other additives and syntheses will also be explored. We suspect that PGS will combine well with several additives and copolymers. Decreasing energy use and testing more environmentally friendly molds are also priorities. Alongside material characterization, PGS-$CaCO_3$ soft robotic designs will be created that utilize single-mold body shapes and more complicated structures.

7 Conclusion

In this work we have introduced the first prototypes of an environmentally benign and degradable soft robot actuator leveraging a biodegradable elastomer. The material synthesis is accessible for those without much experience in chemistry or polymer science, and, elasticity can be varied using the same three chemicals as opposed to buying different formulations of prepared polymers. Also, PGS has been demonstrated in the literature to be fully biodegradable (Rai et al. 2012), so hazardous and long-lasting waste from robot designs is no longer an issue. PGS-$CaCO_3$ will deform and recover under gentle actuation and could be used in biological robots as an organ, muscle, limb or even full body. A green chemistry approach to PGS-$CaCO_3$ synthesis will make workers safer and reduce waste and energy use. Our PGS-$CaCO_3$ synthesis can be performed by roboticists without much prior knowledge of polymer science and improved even further through processing technique and additive exploration, including those that would facilitate 3D printing of the polymer. With the potential to increase soft robot use in data collection, environmental science, and medical technology, PGS-$CaCO_3$ is worth exploring further. We hope that this research inspires other labs to delve into the materials science of their robots to reduce the amount of waste created by this field and explore fascinating impermanent options for robot design.

Acknowledgements The authors thank Dr. Skip Rochefort for his guidance regarding polymer processing and chemistry, and Andrew Brickman, Dylan Thrush and John Morrow IV for equipment assistance.

Compliance with ethical standards

Conflict of interest No competing financial interests exist.

Appendix

Equipment

Equipment: Regulator: Smith, for Nitrogen tank
Flow Meter: Dwyer RMA-150-SSV
Hot Plate: IKA C-MAG HS 7
PTFE-coated liner: Linden Sweden–Jonas of Sweden
Metal baking pan: Nordic Ware
Vacuum oven: VWR Scientific 1410
Thermocouple Readers: Amprobe TMD-56
Aluminum reaction block: Scilogex

Tensile testing dimensions

Tensile testing dimensions are based on the ASTM D412 Die D dimension restrictions for height 16 ± 1 mm, width 100 mm minimum, gauge length 33 ± 2 mm, and large curvature radius 16 ± 2 mm (Fig. 12). The gauge width was kept wider than the Die D dimension of 3 mm to reduce chances of excess stretching while peeling and handling the samples.

Leakage and failure

Photos from leakage and failure testing are shown in Fig. 13.

Motion capture

Motion capture markers were placed on two of the four chambers of Actuator B, two markers per chamber. The grid was drawn by hand with a permanent marker and a ruler using 0.5 cm spacing. The actuator's pressure was increased from 0 to 6.9 kPa evenly across 22 s using a

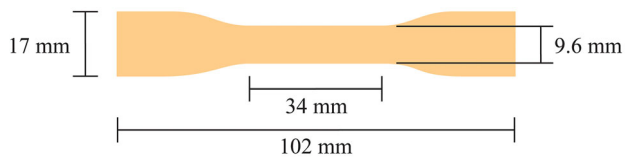

Fig. 12 Tensile and cyclic loading were performed with dumbbell shaped PGS-$CaCO_3$ samples of this size. Sheet thickness of PGS-$CaCO_3$ ranged from approximately 2.6–3.8 mm

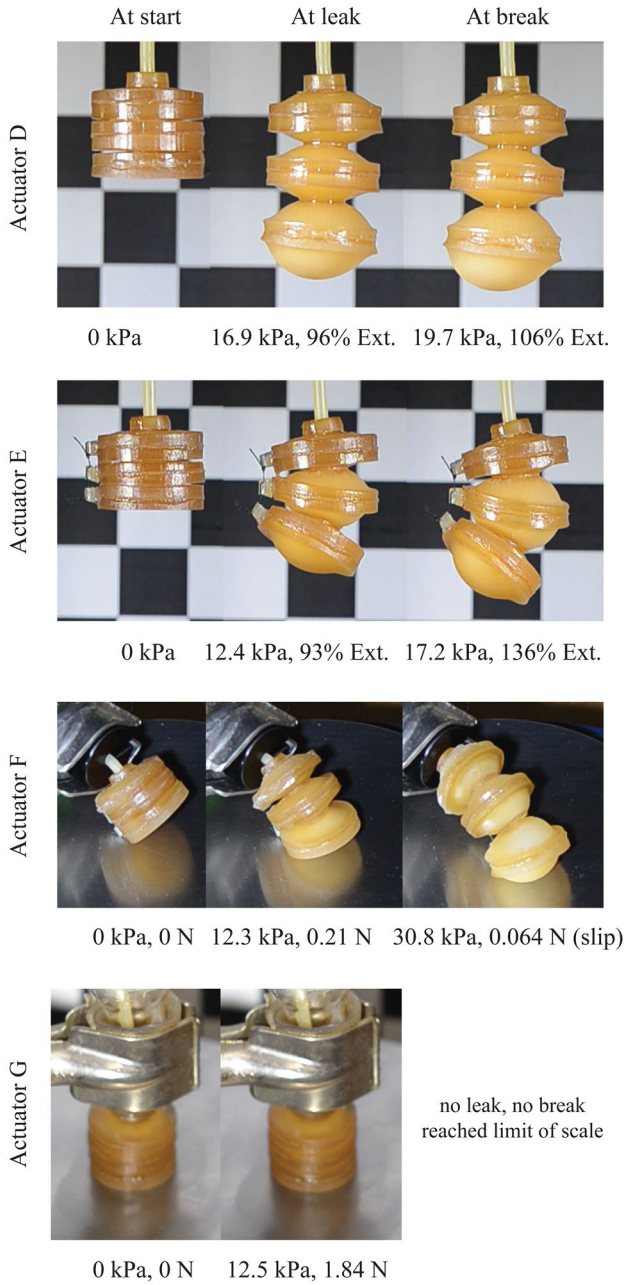

Fig. 13 Failure tests for Actuators D, E, F, and G. Extension at failure ranged from 106% at 19.7 kPa to 136% at 17.2 kPa, and failure for force applied ranged from 1.84 N at 12.5 kPa to 0.064 N at 30.8 kPa due to slipping of the curved actuator

syringe controlled by hand. The motion was recorded both by a four-camera OptiTrak system and a Nikon D7000 camera looking down towards the sample. The locations of the markers in the 2D camera image were found automatically; the grid points were located manually on every 30th frame. The 2D data was aligned to the 3D data by solving for the camera location using the known 2D and 3D locations of the OptiTrak markers, and initial depth of the 2D grid by approximating the actuator's geometry with a

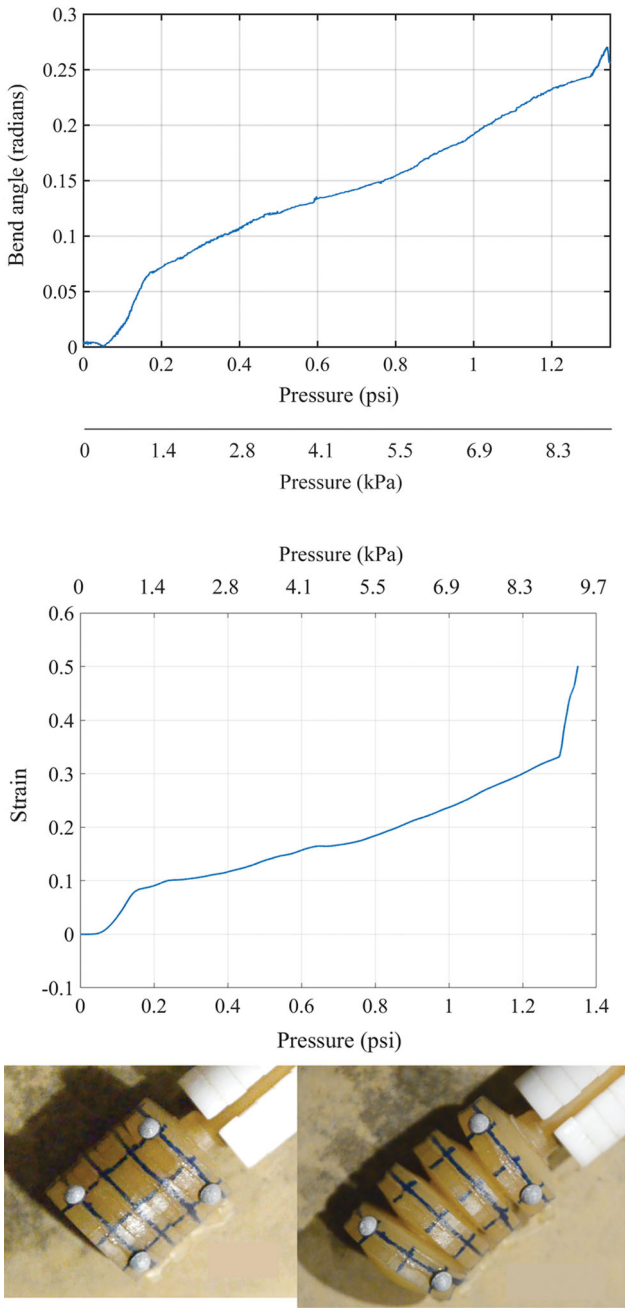

Fig. 14 Motion captured data of the bend and strain vs. pressure for a four-chambered actuator. The sharp slope at approximately 1.4 kPa is due to the slippage of the actuator on the table

cylinder. The 3D data was mapped to a canonical cylinder by finding the rigid body transformation that minimized the difference between the OptiTrak points and canonical matching points on the cylinder.

Bend was calculated by taking the angle between the two markers on the bottom chamber and the two on the top; bend is the angle along the cylinder axis. Extension was calculated by taking the average between each of the points on each chamber and then taking the midpoint between the two separate chambers.

The motion capture data for Actuator B is plotted in Fig. 14. All data is plotted with respect to the pressure. The sharp slope at approximately 1.4 kPa is due to the slippage of the actuator on the table. The elongation of the actuator is slightly nonlinear with increasing pressure, but this could be due to the slipping of the actuator or uneven air flow from the pushed syringe.

Compression testing

Compression testing was performed on 20 mm diameter circular samples using the Mark-10. Samples were placed on top of sandpaper slightly larger than 20 mm in diameter on top of the bottom compression plate. The top compression plate applied force at a constant rate of 3 mm/min until the center of the sample was reached and then traveled upwards at 3 mm/min to complete one cycle. The first three cycles of compression per sample are plotted.

Compression testing results are shown in the Fig 15. The three samples represent the overall spread of data. The samples overlapped and reached force values from 170 to 246 N at 50% strain.

CO_2 Calculation

Calculation of CO_2 release should all $CaCO_3$ dissociate:

Molar mass $CaCO_3$ = 100.0869 g/mol

Ideal mass of $CaCO_3$ going into melt = 0.476 g

0.00476 moles of $CaCO_3$ in = 0.00476 moles of CO_2 out = 0.2095 g CO_2 out

"19.64 pounds of carbon dioxide (CO_2) are produced from burning a gallon of gasoline that does not contain ethanol"

(http://www.eia.gov/tools/faqs/faq.cfm?id=307&t=11)

19.64 lbs CO_2/gal burned = 8909 g CO_2/gal burned

Assuming your car gets 30 miles/gallon, burn 297 g/mile

297 g/mile / 5280 ft/mile = 0.05625 g/ft

0.2095 g CO_2 from polymer/0.05625 g/ft = 3.724 ft

1000 sheets of polymer (approximately 1000 small actuators) = 3724 ft = 0.705 miles

Preparation of natural latex rubber and silicone tensile samples

Natural rubber centrifuged latex (in water) from Liquid Latex Fashions (clear) was poured into a sheet mold and left to dry for 5 days. The rubber sheet was then laser cut with the same laser settings as PGS-$CaCO_3$ and in the same size dumbbells as the PGS-$CaCO_3$. The rubber sheet thicknesses ranged from 1.4 to 1.7 mm.

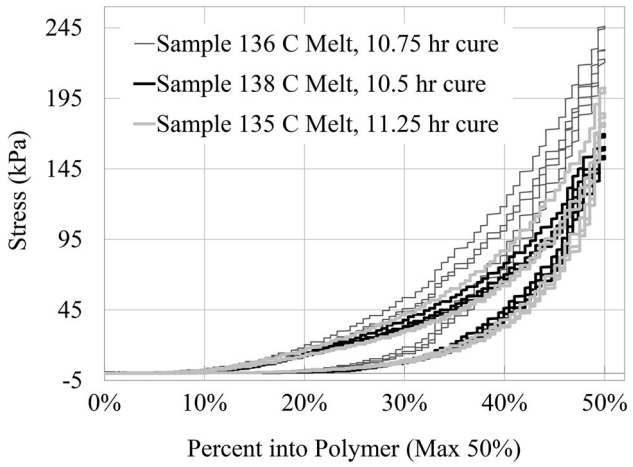

Fig. 15 Compression testing for three samples of different processing conditions and ages. Each sample underwent three compressive cycles at 3 mm/min to 50% of the polymer height. These three samples represent the overall spread of data, and reached from 170 to 246 N

50 wt% Part A and 50 wt% Part B of Ecoflex 00-30 were mixed at 2000 rpm for 30 s and then 2200 rpm for 30 s in a Thinky. The mixture was then poured into the same dumbbell shaped molds as the rubber samples (after mold cleaning) and intermittently vacuumed for 15 min in a vacuum chamber to remove any bubbles. The samples were then placed in a 60 °C oven for 20 min. After being taken out of the oven, sandpaper was glued to the edges of each dumbbell on each side to reduce slipping during testing. The Ecoflex dumbbell thicknesses ranged from 2.3 to 2.9 mm. There was a slight lip on the outer edges of the dumbbell where the silicone met the acrylic mold, so dumbbell thickness was determined using the center of each sample.

References

Anastas, P.T., Warner, J.C.: Green Chemistry: Theory and Practice. Oxford University Press, Oxford [England], New York (1998)

Avantor Performance Materials, Inc.: Safety Data Sheet Calcium Carbonate, Avantor Performance Materials (2014a). https://www.avantormaterials.com/documents/MSDS/usa/sap/00002948.pdf

Bauer, S., Bauer-Gogonea, S., Graz, I., Kaltenbrunner, M., Keplinger, C.: Schwödiauer, R.:25th Anniversary article: A soft future: from robots and sensor skin to energy harvesters. Adv. Mater. **26**(1), 149–162 (2014). doi:10.1002/adma.201303349

Bellingham, C.M., Lillie, M.A., Gosline, J.M., Wright, G.M., Starcher, B.C., Bailey, A.J., Woodhouse, K.A., Keeley, F.W.: Recombinant human elastin polypeptides self-assemble into biomaterials with elastin-like properties. Biopolymers **70**(4), 445–455 (2003). doi:10.1002/bip.10512

Breger, J.C., Yoon, C., Xiao, R., Kwag, H.R., Wang, M.O., Fisher, J.P., Nguyen, T.D., Gracias, H.: Self-folding thermo-magnetically responsive soft microgrippers. ACS Appl. Mater. Interfaces **7**(5), 3398–3405 (2015). doi:10.1021/am508621s

Chambers, L.D., Winfield, J., Ieropoulos, I., Rossiter, J.: Biodegradable and edible gelatine actuators for use as artificial muscles. In: SPIE Smart Structures and Materials+ Nondestructive Evaluation and Health Monitoring (International Society for Optics and Photonics, pp. 90,560B–90,560B (2014) http://proceedings.spiedigitallibrary.org/proceeding.aspx?articleid=1845843

Chen, Q.Z., Bismarck, A., Hansen, U., Junaid, S., Tran, M.Q., Harding, S.E., Ali, N.N., Boccaccini, A.R.: Characterisation of a soft elastomer poly(glycerol sebacate) designed to match the mechanical properties of myocardial tissue. Biomaterials **29**(1), 47–57 (2008doi:10.1016/j.biomaterials.2007.09.010. http://www.sciencedirect.com/science/article/pii/S0142961207007156

Chen, F.J., Dirven, S., Xu, W.L., Li, X.N.: Soft actuator mimicking human esophageal peristalsis for a swallowing robot. IEEE/ASME Trans. Mechatron. **19**(4), 1300–1308 (2014). doi:10.1109/TMECH.2013.2280119. http://ieeexplore.ieee.org/lpdocs/epic03/wrapper.htm?arnumber=6600781

Chen, G., Fu, L., Pham, M.T., Redarce, T.: Characterization and modeling of a pneumatic actuator for a soft continuum robot. In: 2013 IEEE International Conference on Mechatronics and Automation (ICMA) (2013), pp. 243–248. 10.1109/ICMA.2013.6617925

Chen, Q.Z., Ishii, H., Thouas, G.A., Lyon, A.R., Wright, J.S., Blaker, J.J., Chrzanowski, W., Boccaccini, A.R., Ali, N.N., Knowles, J.C., Harding, S.E.: An elastomeric patch derived from poly(glycerol sebacate) for delivery of embryonic stem cells to the heart. Biomaterials **31**(14), 3885–3893 (2010). doi:10.1016/j.biomaterials.2010.01.108. http://www.sciencedirect.com/science/article/pii/S0142961210001407

Chou, C.P., Hannaford, B.: Measurement and modeling of McKibben pneumatic artificial muscles. IEEE Trans. Robot. Autom. **12**(1), 90–102 (1996). doi:10.1109/70.481753

Committee on Prosthetics Research and Development.: The application of external power in prosthetics and orthotics. National Academy of Sciences, National Research Council, Washington DC, Publication 874, (1961)

Davis, S., Tsagarakis, N., Canderle, J., Caldwell, D.G.: Enhanced modelling and performance in braided pneumatic muscle actuators. Int. J. Robot. Res. **22**(3–4), 213–227 (2003). doi:10.1177/0278364903022003006. http://ijr.sagepub.com/content/22/3-4/213

Dobson, R., Gray, V., Rumbold, K.: Microbial utilization of crude glycerol for the production of value-added products. J. Ind. Microbiol. Biotechnol. **39**(2), 217–226 (2012). doi:10.1007/s10295-011-1038-0

Dow Corning: Fascinating Silicone ™: Chemistry Corner—environmental degradation—how polydimethylsiloxane degrades in the environment (2017). http://www.dowcorning.com/content/discover/discoverchem/how-si-degrades.aspx

Flinn Scientific, Inc.: Material Safety Data Sheet Vinegar, Flinn Scientific, Inc. (2012). http://www.flinnsci.com/Documents/MSDS/UV/Vinegar.pdf

Fu, Y., Kao, W.J.: Drug release kinetics and transport mechanisms of non-degradable and degradable polymeric delivery systems. Expert Opin. Drug Deliv. **7**(4), 429–444 (2010). doi:10.1517/17425241003602259. http://www.ncbi.nlm.nih.gov/pmc/articles/PMC2846103/

Fusco, S., Sakar, M.S., Kennedy, S., Peters, C., Bottani, R., Starsich, F., Mao, A., Sotiriou, G.A., Pané, S., Pratsinis, S.E., Mooney, D., Nelson, B.J.: An integrated microrobotic platform for on-demand. targeted therapeutic interventions. Adv. Mater. **26**(6), 952–957 (2014). doi:10.1002/adma.201304098

Global Safety Management.: Safety Data Sheet Vinegar, Fisher Scientific (2014b). https://www.fishersci.com/content/dam/

fishersci/en_US/documents/programs/education/regulatory-documents/sds/chemicals/chemicals-v/S25623.pdf

Glycerol MSDS, Sigma-Aldrich (2016). http://www.sigmaaldrich.com/MSDS/MSDS/DisplayMSDSPage.do?country=US&language=en&productNumber=G7893&brand=SIAL&PageToGoToURL=http%3A%2F%2Fwww.sigmaaldrich.com%2Fcatalog%2Fsearch%3Fterm%3Dglycerol%26interface%3DAll%26N%3D0%2B%26mode%3Dpartialmax%26lang%3Den%26region%3DUS%26focus%3Dproduct

Guan, J., Sacks, M.S., Beckman, E.J., Wagner, W.R.: Synthesis, characterization, and cytocompatibility of elastomeric, biodegradable poly(ester-urethane)ureas based on poly(caprolactone) and putrescine. J. Biomed. Mater. Res. **61**(3), 493–503 (2002). doi:10.1002/jbm.10204

Han, L., Dai, J., Zhang, L., Ma, S., Deng, J., Zhang, R., Zhu, J.: Diisocyanate free and melt polycondensation preparation of bio-based unsaturated poly(ester-urethane)s and their properties as UV curable coating materials. RSC Adv. **4**(90), 49471–49477 (2014). doi:10.1039/C4RA08665A. http://pubs.rsc.org/en/content/articlelanding/2014/ra/c4ra08665a

Ho, V.A., Dao, D.V., Sugiyama, S., Hirai, S.: Development and analysis of a sliding tactile soft fingertip embedded with a microforce/moment sensor. IEEE Trans. Robot. **27**(3), 411–424 (2011). doi:10.1109/TRO.2010.2103470

Ilievski, F., Mazzeo, A.D., Shepherd, R.F., Chen, X., Whitesides, G.M.: Soft robotics for chemists. Angew. Chem. Int. Ed. **50**(8), 1890–1895 (2011). doi:10.1002/anie.201006464. http://onlinelibrary.wiley.com/doi/10.1002/anie.201006464/abstract

Jaafar, I.H., Ammar, M.M., Jedlicka, S.S., Pearson, R.A., Coulter, J.P.: Spectroscopic evaluation, thermal, and thermomechanical characterization of poly(glycerol-sebacate) with variations in curing temperatures and durations. J. Mater. Sci. **45**(9), 2525–2529 (2010). doi:10.1007/s10853-010-4259-0

Jones, J.R.: Review of bioactive glass: from Hench to hybrids. Acta Biomater. **9**(1), 4457–4486 (2013). 10.1016/j.actbio.2012.08.023. http://www.sciencedirect.com/science/article/pii/S1742706112003996

Kharaziha, M., Nikkhah, M., Shin, S.R., Annabi, N., Masoumi, N., Gaharwar, A.K., Camci-Unal, G., Khademhosseini, A.: PGS:Gelatin nanofibrous scaffolds with tunable mechanical and structural properties for engineering cardiac tissues. Biomaterials **34**(27), 6355–6366 (2013). doi:10.1016/j.biomaterials.2013.04.045

Kier, W.M., Smith, K.K.: Tongues, tentacles and trunks: the biomechanics of movement in muscular-hydrostats. Zool. J. Linn. Soc. **83**(4), 307–324 (1985). doi:10.1111/j.1096-3642.1985.tb01178.x

Krishnan, V., Lakshmi, T.: Bioglass: a novel biocompatible innovation. J. Adv. Pharm. Technol. Res. **4**(2), 78–83 (2013). doi:10.4103/2231-4040.111523. http://www.ncbi.nlm.nih.gov/pmc/articles/PMC3696226/

Laubie, B., Ohannessian, A., Desjardin, V., Germain, P.: Methodology to assess silicone (bio)degradation and its effects on microbial diversity. J. Polym. Environ.**20**(4), 1019–1026 (2012). doi:10.1007/s10924-012-0501-y

Li, Y., Thouas, G.A., Chen, Q.Z.: Biodegradable soft elastomers: synthesis/properties of materials and fabrication of scaffolds. RSC Adv. **2**(22), 8229–8242 (2012). doi:10.1039/C2RA20736B. http://pubs.rsc.org.ezproxy.proxy.library.oregonstate.edu/en/content/articlelanding/2012/ra/c2ra20736b

Liang, S.L., Cook, W.D., Thouas, G.A., Chen, Q.Z.: The mechanical characteristics and in vitro biocompatibility of poly(glycerol sebacate)-Bioglass- elastomeric composites. Biomaterials **31**(33), 8516–8529 (2010). doi:10.1016/j.biomaterials.2010.07.105. http://www.sciencedirect.com/science/article/pii/S0142961210009774

Liang, S., Cook, W.D., Chen, Q.: Physical characterization of poly(glycerol sebacate)/bioglass-composites. Polym. Int. **61**(1), 17–22 (2012). doi:10.1002/pi.3165

Mac Murray, B.C., An, X., Robinson, S.S., van Meerbeek, I.M., O'Brien, K.W., Zhao, H., Shepherd, R.F.: Poroelastic foams for simple fabrication of complex soft robots. Adv. Mater. **27**(41), 6334–6340, (2015). doi:10.1002/adma.201503464

Martinez, R.V., Branch, J.L., Fish, C.R., Jin, L., Shepherd, R.F., Nunes, R.M.D., Suo, Z., Whitesides, G.M.: Robotic tentacles with three-dimensional mobility based on flexible elastomers. Adv. Mater. **25**(2), 205–212 (2013). doi:10.1002/adma.201203002

Miyashita, S., Guitron, S., Ludersdorfer, M., Sung, C., Rus, D.: An untethered miniature origami robot that self-folds, walks, swims, and degrades. In: 2015 IEEE International Conference on Robotics and Automation (ICRA) (2015), pp. 1490–1496. doi:10.1109/ICRA.2015.7139386

Morin, S.A, Shevchenko, Y., Lessing, J., Kwok, S.W., Shepherd, R.F., Stokes, A.A., Whitesides, G.M.: Using click-e-bricks to make 3D elastomeric structures. Adv. Mater. **26**, 5991–5999 (2014a). http://gmwgroup.harvard.edu/pubs/pdf/1220.pdf

Morin, S.A., Kwok, S.W., Lessing, J., Ting, J., Shepherd, R.F., Stokes, A.A., Whitesides, G.M.: Elastomeric tiles for the fabrication of inflatable structures. Adv. Funct. Mater. **24**, 5541–5549 (2014b)

Mosadegh, B., Polygerinos, P., Keplinger, C., Wennstedt, S., Shepherd, R.F., Gupta, U., Shim, J., Bertoldi, K., Walsh, C.J., Whitesides, G.M.: Pneumatic networks for soft robotics that actuate rapidly. Ad. Funct. Mater. **24**(15), 2163–2170 (2014). doi:10.1002/adfm.201303288

Mulla, D.J.: Twenty five years of remote sensing in precision agriculture: Key advances and remaining knowledge gaps. Biosyst. Eng. **114**(4), 358–371 (2013). doi:10.1016/j.biosystemseng.2012.08.009. http://www.sciencedirect.com/science/article/pii/S1537511012001419

Murphy, R.R., Peschel, J., Arnett, C., Martin, D.: Projected needs for robot-assisted chemical, biological, radiological, or nuclear (CBRN) incidents. In: 2012 IEEE International Symposium on Safety, Security, and Rescue Robotics (SSRR) (2012), pp. 1–4. 10.1109/SSRR.2012.6523881

Muscato, G., Bonaccorso, F., Cantelli, L., Longo, D., Melita, C.D.: Volcanic environments: robots for exploration and measurement. IEEE Robot. Autom. Mag. **19**(1), 40–49 (2012). doi:10.1109/MRA.2011.2181684

Nijst, C.L.E., Bruggeman, J.P., Karp, J.M., Ferreira, L., Zumbuehl, A., Bettinger, C.J., Langer, R.: Synthesis and Characterization of Photocurable Elastomers from Poly(glycerol-*co*-sebacate). Biomacromolecules **8**(10), 3067–3073 (2007). doi:10.1021/bm070423u. http://www.ncbi.nlm.nih.gov/pmc/articles/PMC2662850/

Ogunniyi, D.S.: Castor oil: a vital industrial raw material. Bioresource Technology **97**(9), 1086–1091 (2006). doi:10.1016/j.biortech.2005.03.028. http://www.sciencedirect.com/science/article/pii/S0960852405002026

Oregon: Environmental toxicology section. calcium carbonate "lime, Limewater". Health Effects Information (1998) http://library.state.or.us/repository/2008/200808011132585/

Patel, A., Gaharwar, A.K., Iviglia, G., Zhang, H., Mukundan, S., Mihaila, S.M., Demarchi, D., Khademhosseini, A.: Highly elastomeric poly(glycerol sebacate)-co-poly(ethylene glycol) amphiphilic block copolymers. Biomaterials **34**(16), 3970–3983 (2013). doi:10.1016/j.biomaterials.2013.01.045

Quispe, C.A.G., Coronado, C.J.R., Carvalho Jr., J.A.: Glycerol: production, consumption, prices, characterization and new trends in combustion. Renew. Sustain. Energy Rev. **27**, 475–493 (2013). doi:10.1016/j.rser.2013.06.017.http://www.sciencedirect.com/science/article/pii/S1364032113003948

Rai, R., Tallawi, M., Grigore, A., Boccaccini, A.R.: Topical issue on biorelated polymers. Prog. Polym. Sci. **37**(8), 1051–1078 (2012). doi:10.1016/j.progpolymsci.2012.02.001. http://www.sciencedirect.com/science/article/pii/S0079670012000172

Ratner, B.D., Hoffman, A.S., Schoen, F.J., Lemons, J.E.: Biomaterials Science: An Introduction to Materials in Medicine. Academic Press, Boston (2004)

Roy Olsson.: Inbound, Controlled, Air-Releasable, Unrecoverable Systems (ICARUS, DARPA) (2017). http://www.darpa.mil/program/inbound-controlled-air-reasonable-unrecoverable-systems

Rus, D., Tolley, M.T.: Design, fabrication and control of soft robots. Nature **521**(7553), 467–475 (2015). doi:10.1038/nature14543. http://www.nature.com.ezproxy.proxy.library.oregonstate.edu/nature/journal/v521/n7553/full/nature14543.html

Saltzman, W.M.: Drug Delivery: Engineering Principles for Drug Therapy. Oxford University Press, New York (2001)

Saltzman, W.M.: Tissue Engineering: Engineering Principles for the Design of Replacement Organs and Tissues. Oxford University Press, New York (2004)

Sebacic Acid Material Safety Data Sheet, Sigma Aldrich (2015). http://www.sigmaaldrich.com/MSDS/MSDS/DisplayMSDSPage.do?country=US&language=en&productNumber=283258&brand=ALDRICH&PageToGoToURL=http:%3A%2F%2Fwww.sigmaaldrich.com%2Fcatalog%2Fproduct%2Faldrich%2F283258%3Flang%3Den

Shankar, R., Ghosh, T.K., Spontak, R.J.: Dielectric elastomers as next-generation polymeric actuators. Soft Matter **3**(9), 1116 (2007). doi:10.1039/b705737ghttp://xlink.rsc.org/?DOI=b705737g

Shepherd, R.F., Ilievski, F., Choi, W., Morin, S.A., Stokes, A.A., Mazzeo, A.D., Chen, X., Wang, M., Whitesides, G.M.: Multigait soft robot. Proc. Natl. Acad. Sci. **108**(51), 20400–20403 (2011). doi:10.1073/pnas.1116564108. http://www.pnas.org/content/108/51/20400

Shian, S., Bertoldi, K., Clarke, D.R.: Dielectric elastomer based grippers for soft robotics. Adv. Mater. **27**(43), 6814–6819 (2015). doi:10.1002/adma.201503078

Stoica A.: Advanced Technologies for Enhanced Quality of Life, 2009. AT-EQUAL '09. (2009), pp. 47–51. 10.1109/AT-EQUAL.2009.46

Stokes, A.A., Shepherd, R.F., Morin, S.A., Ilievski, F., Whitesides, G.M.: A hybrid combining hard and soft robots. Soft Robot. **1**(1), 70–74 (2014). doi:10.1089/soro.2013.0002

Sun, Z.J., Wu, L., Huang, W., Chen, C., Chen, Y., Lu, X.L., Zhang, X.L., Yang, B.F., Dong, D.L.: Glycolic acid modulates the mechanical property and degradation of poly(glycerol, sebacate, glycolic acid. J. Biomed. Mater. Res. Part A **92**(1), 332–339 (2010). doi:10.1002/jbm.a.32370

Suprem, A., Mahalik, N., Kim, K.: A review on application of technology systems, standards and interfaces for agriculture and food sector. Comput. Stand. Interfaces **35**(4), 355–364 (2013). doi:10.1016/j.csi.2012.09.002. http://www.sciencedirect.com/science/article/pii/S0920548912000955

The Dow Chemical Company.: Product Safety Assessment, DOW Acrylic Acid (2014). http://msdssearch.dow.com/PublishedLiteratureDOWCOM/dh_0926/0901b803809269b6.pdf?filepath=productsafety/pdfs/noreg/233-00269.pdf&fromPage=GetDoc

Thomas, L.V., Nair, P.D.: (Citric acidcopolycaprolactone triol) polyester. Biomatter **1**(1), 81–90 (2011). doi:10.4161/biom.1.1.17301. http://www.ncbi.nlm.nih.gov/pmc/articles/PMC3548247/

Trimmer, B., Lin, H.T., Baryshyan, A., Leisk, G., Kaplan, D.L.: Towards a biomorphic soft robot: Design constraints and solutions In: 2012 4th IEEE RAS EMBS International Conference on Biomedical Robotics and Biomechatronics (BioRob) (2012), pp. 599–605. doi:10.1109/BioRob.2012.6290698

Valdes, S., Urza, I., Pounds, P., Singh, S.: Samara: low-cost deployment for environmental sensing using passive autorotation. In: Robotics: Science and Systems Workshop on Robotics for Environmental Monitoring, Citeseer (2012). http://citeseerx.ist.psu.edu/viewdoc/download?doi=10.1.1.470.4128&rep=rep1&type=pdf

Wang, Y., Ameer, G.A., Sheppard, B.J., Langer, R.: A tough biodegradable elastomer. Nat. Biotechnol. **20**(6), 602, (2002). http://proxy.library.oregonstate.edu/login?url=http://search.ebscohost.com/login.aspx?direct=true&db=aph&AN=8782426&site=ehost-live

Xu, C., Xu, C., Zheng, J.: A novel dielectric elastomer actuator based on polyvinyl alcohol hydrogel electrodes. arXiv preprint arXiv:1409.2611 (2014)

Yang, J., Webb, A., Ameer, G.: Novel citric acid-based biodegradable elastomers for tissue engineering. Adv. Mater. **16**(6), 511–516 (2004). doi:10.1002/adma.200306264

Stephanie Walker is a dual Ph.D. student in Materials Science and Robotics at Oregon State University, and works on polymer material functionality for soft robotics. Her interests are biodegradable materials, fabrication technologies, and soft devices. She received her B.S. in Chemical Engineering from Oregon State University and her B.A. in Applied Science (focus in Graphic Design) from San Diego State University.

Jacob Rueben is currently an undergraduate student working towards his B.S. in chemical engineering with a focus on materials science and microelectronics at Oregon State University. His research involves developing UV-curing green materials for use in soft robots.

Tessa Van Volkenburg is currently an undergraduate student studying Chemical Engineering at Oregon State University.

Samantha Hemleben is currently a graduate student at Oregon State University working towards her M.S. in Robotics with a minor in Computer Science. Her research focuses on modeling 3D printed materials.

Dr. Cindy Grimm works in the area of surface modeling and visualization, with an emphasis on biomedical applications. Her current projects include: modeling the developing heart, understanding how the shape of bat ears influences their sonar patterns, 3D sketching, and interfaces for 3D medical image segmentation. She received her PhD from Brown University in 1995 in the area of surface modeling, spent two years working at Microsoft Research on facial animation, then ten years as faculty at Washington University in St. Louis. She is now in the Mechanical Engineering department at Oregon State University.

Dr. John Simonsen received a Ph.D. in Physical Chemistry from the University of Colorado in 1975. He joined the faculty of the Oregon State University (OSU) Department of Forest Products in 1990, following more than a decade of working in small and medium-sized businesses in the chemical industry, including Simonsen Chemical Company, which formulated and sold wood preservatives to the wood treating industry. He is presently a Professor in the Department of Wood Science and Engineering, the OSU Materials Science Program and holds graduate status in the Department of Chemical Engineering. He is also a member of ONAMI (the Oregon Nanoscience and Microtechnologies Institute). Dr. Simonsen's research interests include cellulose chemistry, especially cellulose nanomaterials (CN) and polymer composites, including natural fiber-polymer composites. Investigations have spanned a broad range, from grafting DNA to cellulose nanocrystals (CNCs), developing a variety of CNC-filled polymer composites, carbonized CN for battery anodes, TEM tomography of CNC aerogels, CN-based edible coatings for food, and 3D print materials utilizing CN.

Dr. Yiğit Mengüç received his B.S. degree from Rice University, in 2006, and his M.S. and Ph.D. degrees from the Department of Mechanical Engineering at Carnegie Mellon University, in 2009 and 2011, respectively. He completed his postdoctoral fellowship at the Wyss Institute for Biologically Inspired Engineering at Harvard University in 2014 before joining the Robotics program at Oregon State University (OSU). He leads research into soft robot materials, mechanics, and manufacturing as the founder and director of the mLab at OSU.